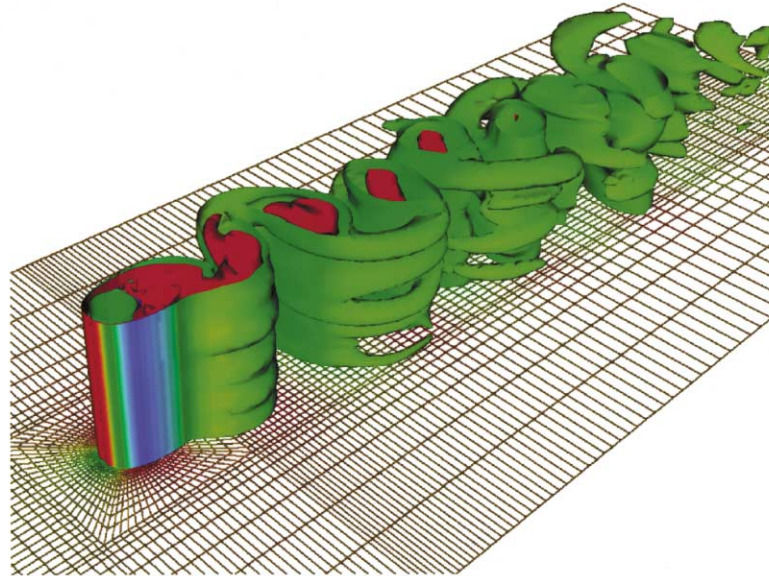


### 1. 3D Simulation of Flow Past a Cylinder at $Re=300$

*Kalro, V.<sup>1)</sup> and Tezduyar, T.<sup>1)</sup>*

*1) Army High Performance Computing Research Center, University of Minnesota  
1100 Washington Avenue South, Suite 101, Minneapolis, Minnesota 55415, U.S.A.*

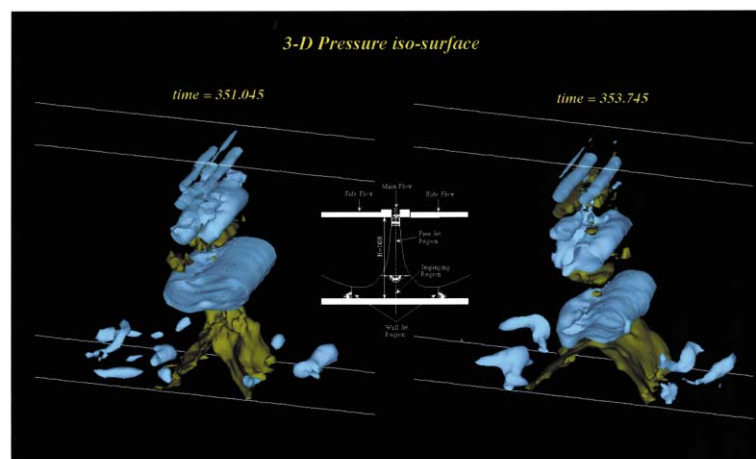


The isosurfaces show the columnar vortices which generate strain fields which interact with neighboring vortices. This causes the vortices to distort and exhibit strong 3D behavior. The outer isosurfaces are color-coded with fluid pressure while the inner ones are just painted red. At each time step, over 760,000 coupled, nonlinear equations are solved. The computation was performed on a 512-node CM-5, using the flow solver developed by the Team for Advanced Flow Simulation and Modeling at the Army HPC Research Center.

### 2. 3D Simulation of the Plane Impinging Jet

*Tsubokura, M.<sup>1)</sup>, Kobayashi, T.<sup>1)</sup> and Taniguchi, N.<sup>1)</sup>*

*1) Institute of Industrial Science, University of Tokyo  
7-22-1, Roppongi, Minatoku, Tokyo 106-8558, Japan*

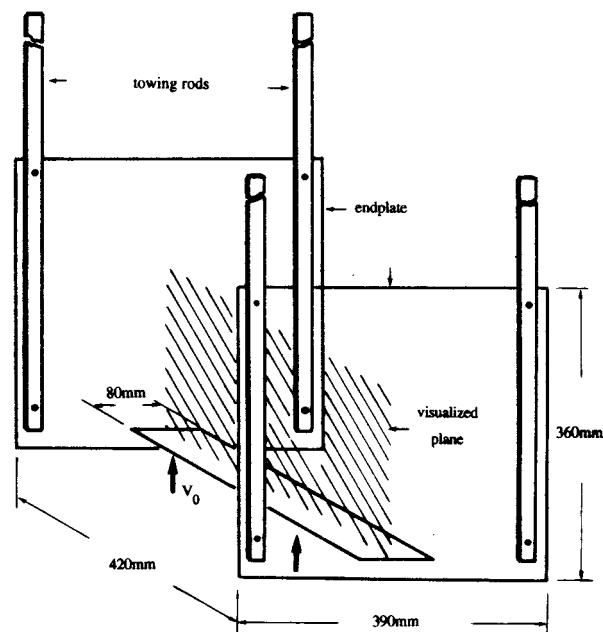
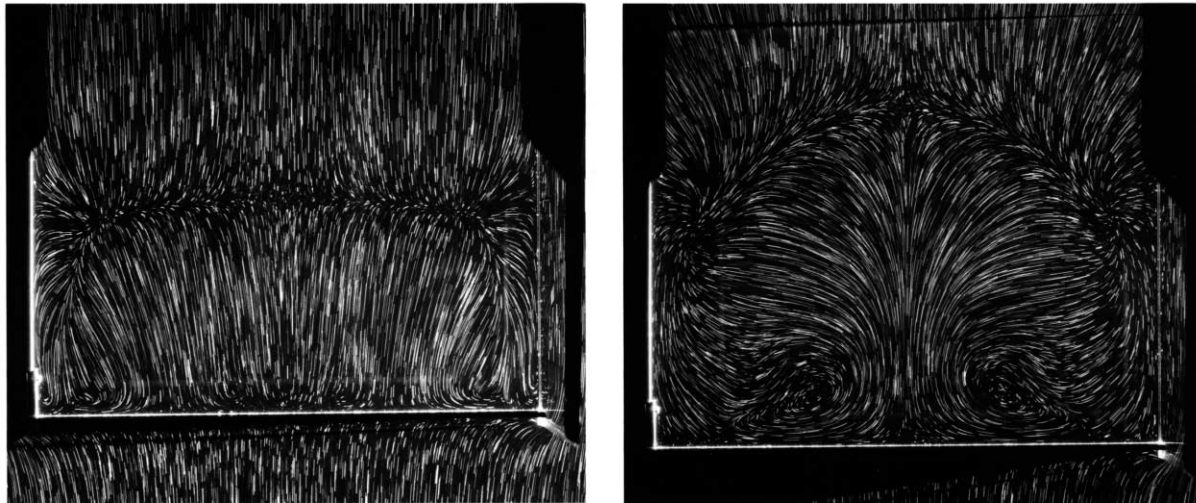


This figure indicates pressure iso-surface of the plane impinging jet at two instants which is numerically simulated by Large Eddy Simulation(LES). Reynolds number normalized by nozzle width and inlet velocity is 6,000. It is shown that pressure field is almost two dimensional just near the nozzle exit region. But after the impinging, fully three dimensional structure is observed. LES is suitable to investigate such organized structures because this method simulates flow field instantaneously at 3D region.

### 3. Setting up of Three-dimensional Endplate Effect on the Starting Wake of a Perpendicular Flat Plate

Coutanceau, M.<sup>1)</sup> and Ehrmann, P.<sup>1)</sup>

1) University of Poitiers, 40 Avenue du Reeteur Pineau, Poitiers, Cedex France 86022



Schematic of the experimental model arrangement.

A thin horizontal(5.2:1) flat plate equipped with endplates is towed uniformly, after an impulsive start, up-to-down in a vertical oil tank. The pictures, taken by an accompanying camera, show two successive spanwise views of the wake structure after the model has travelled along a distance of four and eight plate widths respectively, for a Reynolds number of 200. It is seen how the initial horizontal instream line which separates the reversed flow from the general current (running upwards) becomes with increasing time very incurved and how two perpendicular vortices form near the flat plate (on each photo, the upper parts of the vertical endplate traces are hidden by the forward towing rods).

More details of the way this very strong and complex 3-D endplate effect (however often ignored) sets in with time, as well as its sensivity to the model shape, are shown in Ehrmann thesis(Poitiers 1996).

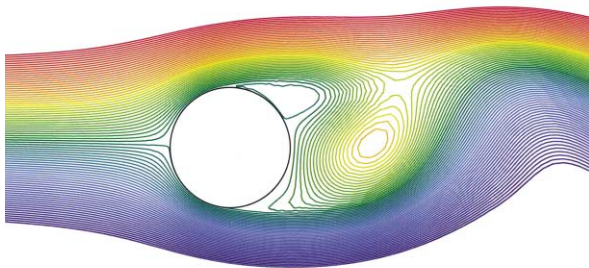
#### 4. Analytical Result of Two-dimensional Cylinder Model

Kimura, Y.<sup>1)</sup>, Aoki, K.<sup>1)</sup>, Oki, M.<sup>2)</sup> and Nakayama, Y.<sup>3)</sup>

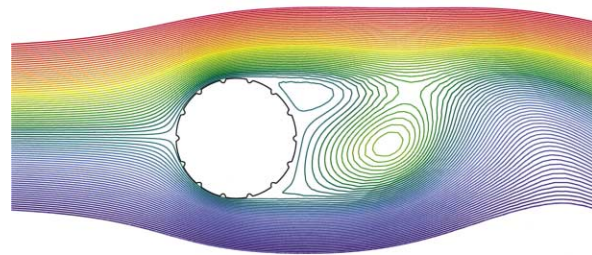
1) Tokai University, 1117 kitakaname, Hiratsuka, Kanagawa, 259-1292, Japan

2) Tokai University, 317 Nishino, Numazu, Shizuoka, 410-0321, Japan

3) Future Technology Research Institute, 3-56-2 Higashi-Oizumi Nerima, Tokyo 178-0063, Japan

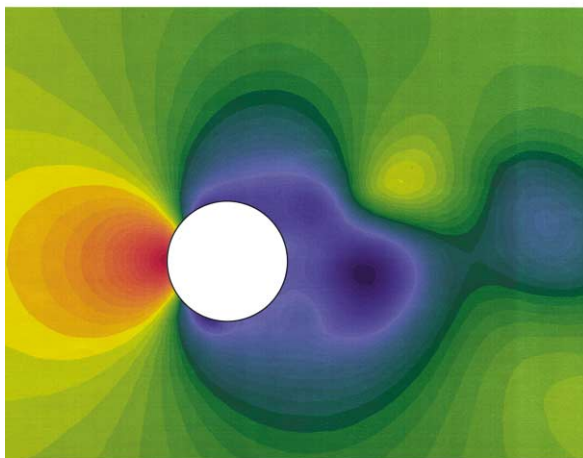


(a) Cylinder with smooth face

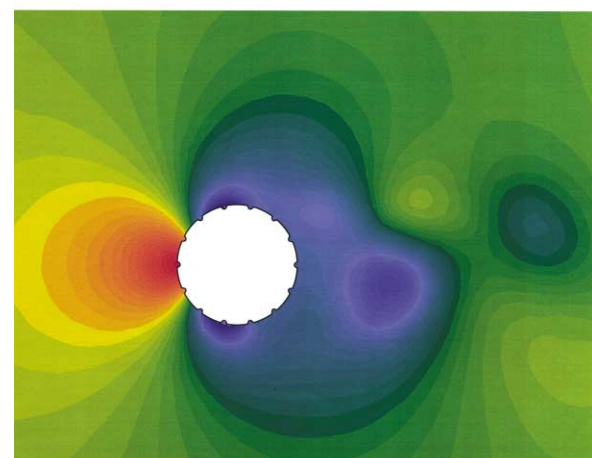


(b) Cylinder with grooves

#### 4.1 Stream lines



(a) Cylinder with smooth face



(b) Cylinder with grooves

#### 4.2 Pressure distribution

4.1 and 4.2 show the results of the unsteady computation conducted for flows around two-dimensional cylinders using RNG  $k-\varepsilon$  models.

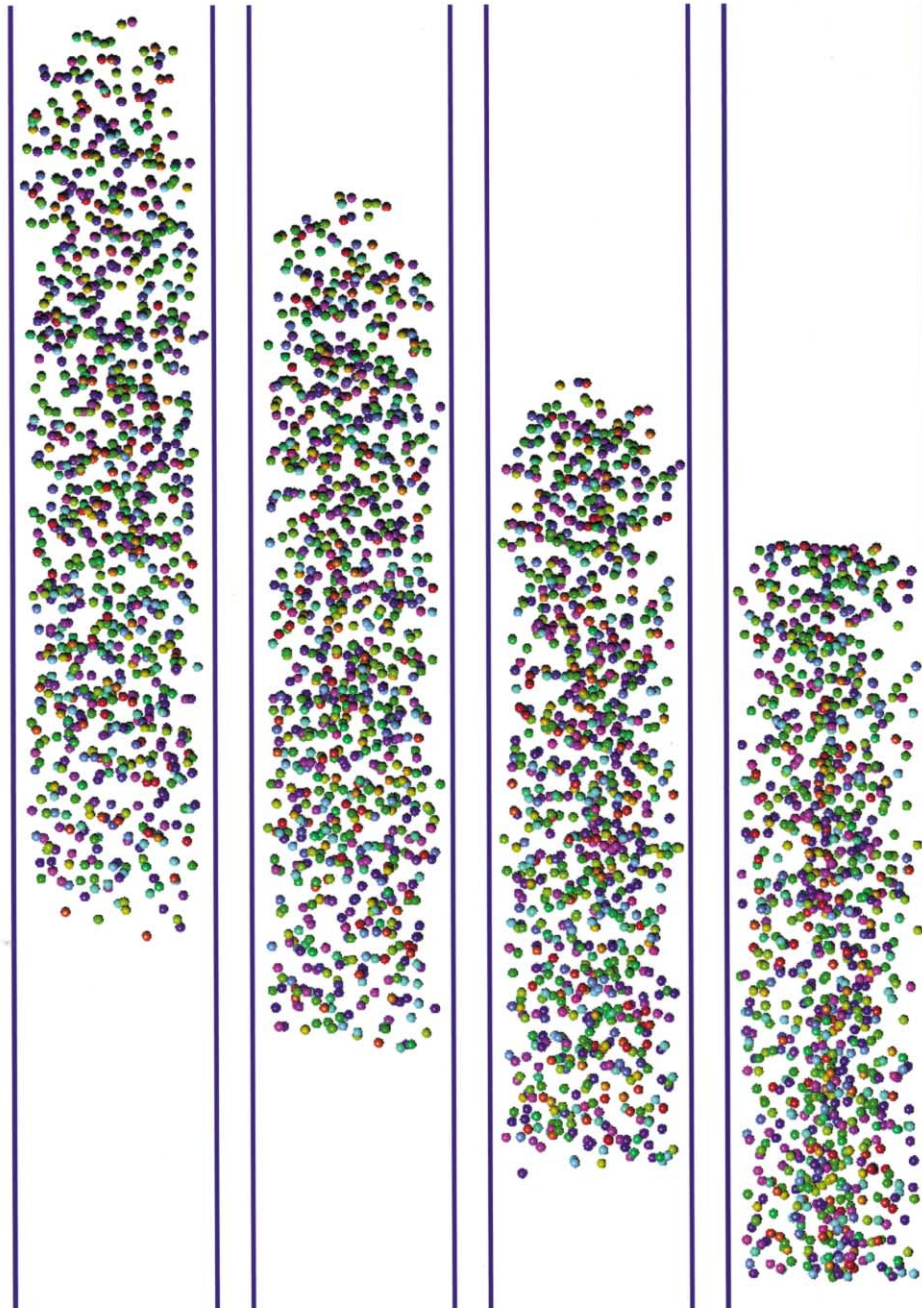
4.1(a) and (b) respectively show the stream lines around a smooth cylinder and another with 14 longitudinal grooves at  $Re=82,500$ . From these figures, it is found that the separation point for a grooved cylinder locates lowerstream than that for a smooth cylinder while the wake region for the former being narrower than that for the latter.

On the other hand, 4.2(a) and (b) respectively show the pressure distribution around the smooth cylinder and the grooved cylinder when  $Re=82,500$ . The pressure of the smooth cylinder in the downstream region is larger than that of the grooved cylinder in the similar region. From these figures, the drag for a grooved is smaller than that for a smooth cylinder.

### 5. 3D Simulation of 1000 Spheres Falling in a Liquid-filled Tube

Johnson, A.<sup>1)</sup> and Tezduyar, T.<sup>1)</sup>

1) Army High Performance Computing Research Center, University of Minnesota  
1100 Washington Avenue South, Suite 101, Minneapolis, Minnesota 55415, U.S.A.

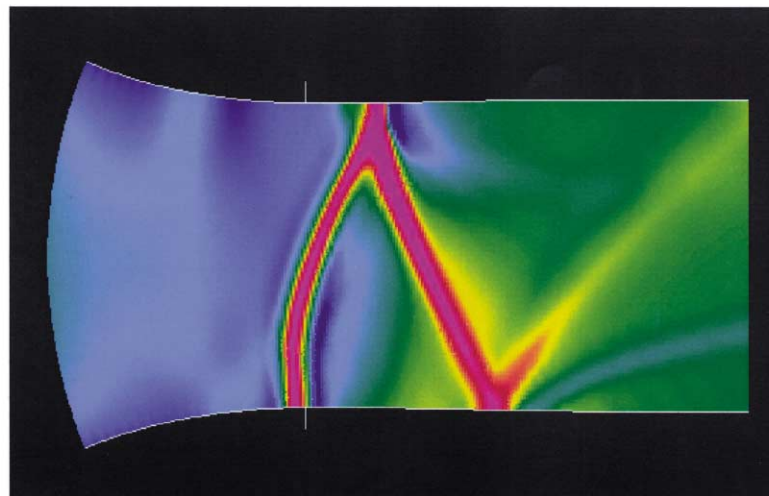
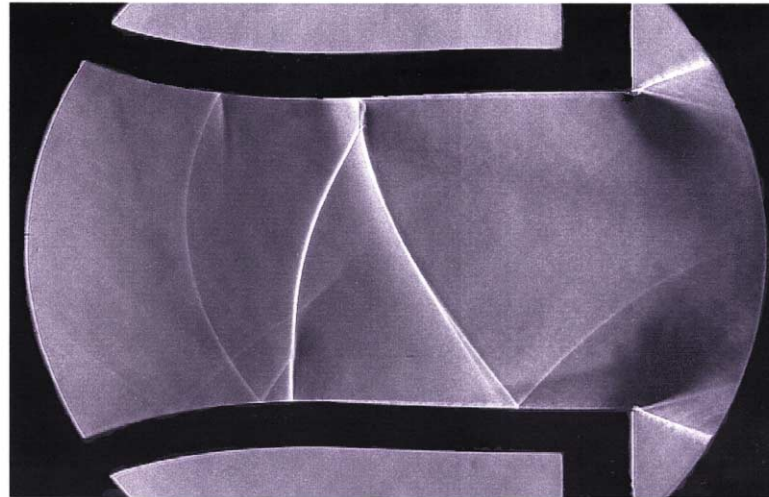


Distribution of the spheres at four instants (including the initial instant). For a single sphere,  $Re=10$ . The colors are for identifying the individual spheres. The simulation was performed, in a multi-platform simulation environment, using a 512-node CM-5 and a 2-processor SGI ONYX2. The flow solution and the mesh generation and update methods were developed by the Team for Advanced Flow Simulation and Modeling at the Army HPC Research Center.

## 6. Inviscid Instability of High Speed Two-phase Flow

Schnerr, G. H.<sup>1)</sup> and Adam, S.<sup>1)</sup>

1) Universität Karlsruhe(TH) Kaiserstrasse 12, D-76128 Karlsruhe, Germany



The schlieren picture shows the unsteady transonic flow of a water vapor/carrier gas mixture through a laval nozzle from left to right. Due to the rapid cooling during the expansion the water vapor becomes highly supersaturated and it condenses suddenly near the throat. This leads to thermal choking with unsteady moving oblique shocks in the symmetric nozzle, the frequency is 832Hz. The perfect agreement of experiment and calculation confirms that this bifurcation phenomenon is a new instability caused by strong interactions of compressibility waves and heat addition in transonic flow, and is definitely not controlled by viscosity effects like boundary layer separation etc.

### Experiment

Fluid	Atmospheric humid air
Reservoir temperature	$T_{0i}=290.3\text{K}$
Reservoir pressure of the mixture	$P_{0i}=1.0\text{bar}$
Water vapor content	10.0g water vapor/kg dry air
Flow visualization	Spark light source Strobokin
	Exposure time 1 $\mu\text{s}$

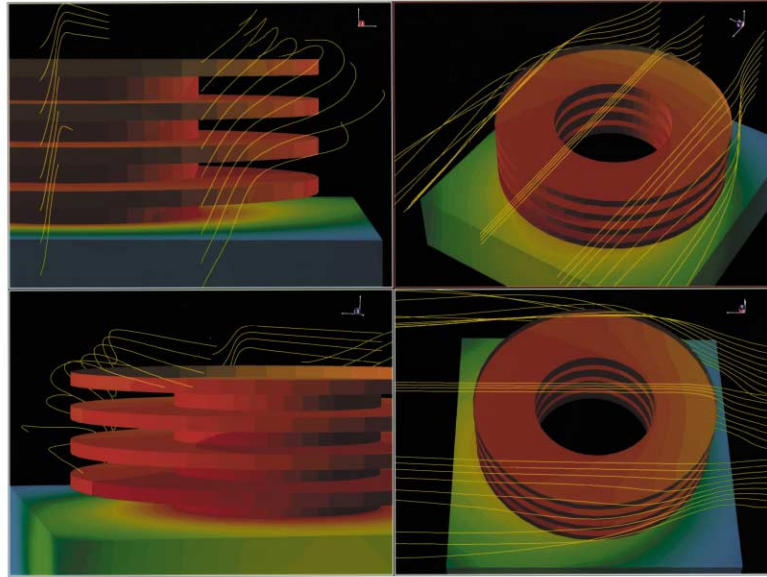
### Calculation

Model	Inviscid-Euler equations
Color scale	Static pressure disturbance

## 7. Electronics Module Cooling

Rifai, S.<sup>1)</sup>

1) Centric Engineering Systems, Inc., 624 East Evelyn Avenue, Sunnyvale, CA 94086, U.S.A.

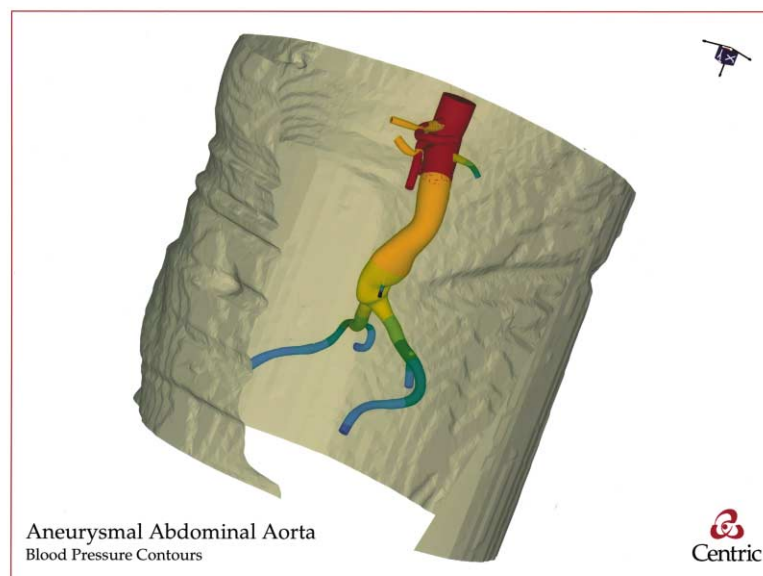


Visualization of the cooling process for an electronics module. Centric's Spectrum(TM) is used for multiphysics simulation and visualization of this thermal management application. The color contours represent the temperature field within a Motorola MCA2800-ALS bipolar gate array. Streamlines of the cooling flow around the module are also shown.

## 8. Vascular Blood Flow Simulation

Taylor, C.<sup>1)</sup>

1) Division of Vascular Surgery, Stanford University, Stanford, CA 94305, U.S.A.



Visualization of a patient's aneurysmal abdominal aorta. Centric's Spectrum(TM) is used to model and visualize pulsatile blood flow within arteries using computational fluid dynamics. The outside surface is the patient's skin, and a clipping plane exposes the aorta. The color contours depict the blood pressure distribution at an instant in time during the pulse cycle.